RSC Advances

This article can be cited before page numbers have been issued, to do this please use: L. Fu, L. Liu, Z. Ruan, H. Zhang and L. Yan, *RSC Adv.*, 2016, DOI: 10.1039/C6RA05657A.

ROYAL SOCIETY OF CHEMISTRY

www.rsc.org/advances

View Article Online
DOI: 10.1039/C6RA05657A

RSC Advances

ARTICLE

Folic Acid Targeted pH-Responsive Amphiphilic Polymer Nanoparticles Conjugated with Near Infrared Fluorescence Probe for Imaging-guided Drug Delivery

Received 00th January 20xx,
Accepted 00th January 20xx

DOI: 10.1039/x0xx00000x

www.rsc.org/

Liyi Fu, Le Liu, Zheng Ruan, Houbing Zhang and Lifeng Yan*

A novel folic acid targeted pH-responsive amphiphilic polymer conjugated with near infrared (NIR) probe has been synthesized by the combination of reversible addition-fragmentation chain transfer (RAFT) polymerization of 2-(N-tert-butoxycarbonylamino)ethyl methacrylate (BEMA) and oligo(ethylene glycol) methacrylate (OEGMA), ring-opening polymerization of N-carboxy anhydride (NCA) and Click Reaction. After assembling to micelles, the polymeric nanoparticles has pH-responsive properties for delivery encapsulated drug into the tumor cell *via* a rapid process of expansion and subsequent disassembly. Folic acid linked to the amino groups on the branched chains would promote the endocytosis of the polymeric nanoparticles by the cells leading the improvement of the effect of doxorubicin (DOX). *In vitro* experiments on both MCF7 and HepG2 cells revealed the as-prepared polymer might be a potential candidate for future theranosic against cancer.

Introduction

Multifunctional nanomaterials, especially focused on targeting, stimuli-response and bioimaging, attracted great attention and have been widely studied recently.[1-3] Plenty of polymers, liposomes or some other nanoparticles were synthesized and characterized to fulfill various demands of targeted delivery,[4,5] stimuli-responsive imaging,[6,7] targeted imaging,[8,9] etc, for the treatment of cancer. Multifunctional nanomaterials and diversified methods improve our comprehension on cancer, and the so-called "theranostic" indicates the importance of the early stage diagnosis and the subsequent directed therapy. So development of novel multifunctional nanomaterial will overcome limitations with conventional diagnosis and therapy and hold great promise for the future of cancer treatment.[10,11]

Targeted polymeric drug delivery system has attracted much attention for it can enhance the enrichment of the polymeric drug nanoparticles in tumor and endocytosis in cells. However, the bioimaging of the target process during the drug delivery is still scare. It is very interesting to develop new imaging-guided targeted polymeric drug delivery system for new theranostics. In our previous work, a galactose targeted pH-responsive copolymer conjugated with a cyanine dye had been synthesized for bioimaging and drug delivery, which showed efficient drug delivery behavior for the liver cancer cells (HepG2).[12] We used galactose to target and obtained satisfied results. Here, we change our strategy to another target group to make our design of multiblock polymer applicable for more cancer cells (Scheme 1). Folic acid (FA), whose folate receptor is overexpressed on the surface of many tumor cells, is considered to be a satisfactory target group against breast cancer, kidney cancer, liver cancer, and ovarian cancer cells,[13,14] while in normal tissues, these receptors have limited distribution.[15] The therapeutic efficacy of folate receptors has been proven by selective accumulation into tumor cells by folate receptor-mediated endocytosis.[16]

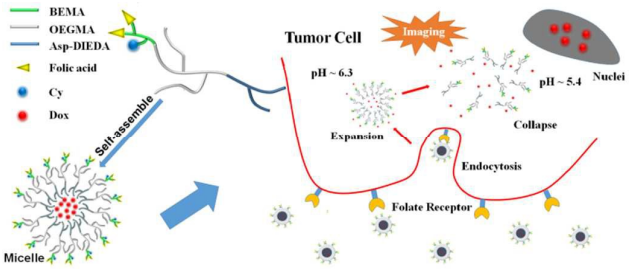

Scheme 1. Diagrammatic sketch ligand targeted polymer conjugated with NIR probe, the micellization with DOX, selective accumulation in cancer cell, and the imaging of the endocytosis of the micelle with subsequent pH triggered drug release

In addition, polypeptides have been studied for decades to construct multiblock amphiphilic copolymers.[17-20] Based on its excellent characters of biocompatibility and biodegradability, polypeptides are widely used in the field of nano-pharmaceutical materials. Polypeptides synthesized by the ring-opening polymerization (ROP) of α-amino acid N-carboxyanhydrides (NCAs) have a satisfactory polydispersity index (PDI) which could be controlled within 1.1 leading a

CAS Key Laboratory of Soft Matter Chemistry, Hefei National Laboratory for Physical Sciences at the Microscale,, iChEM, University of Science and Technology of China. Jinzai Road 96#, Hefei, 230026, Anhui, P.R.China. Fax: (+86-551-63606853); E-mail: (lfyan@ustc.edu.cn).
† Footnotes relating to the title and/or authors should appear here.

View Article Online
DOI: 10.1039/C6RA05657A

narrow size distribution. Also, the side chain of α-amino acid (lysine, aspartic acid, etc) offers different sites for the demands of modification.

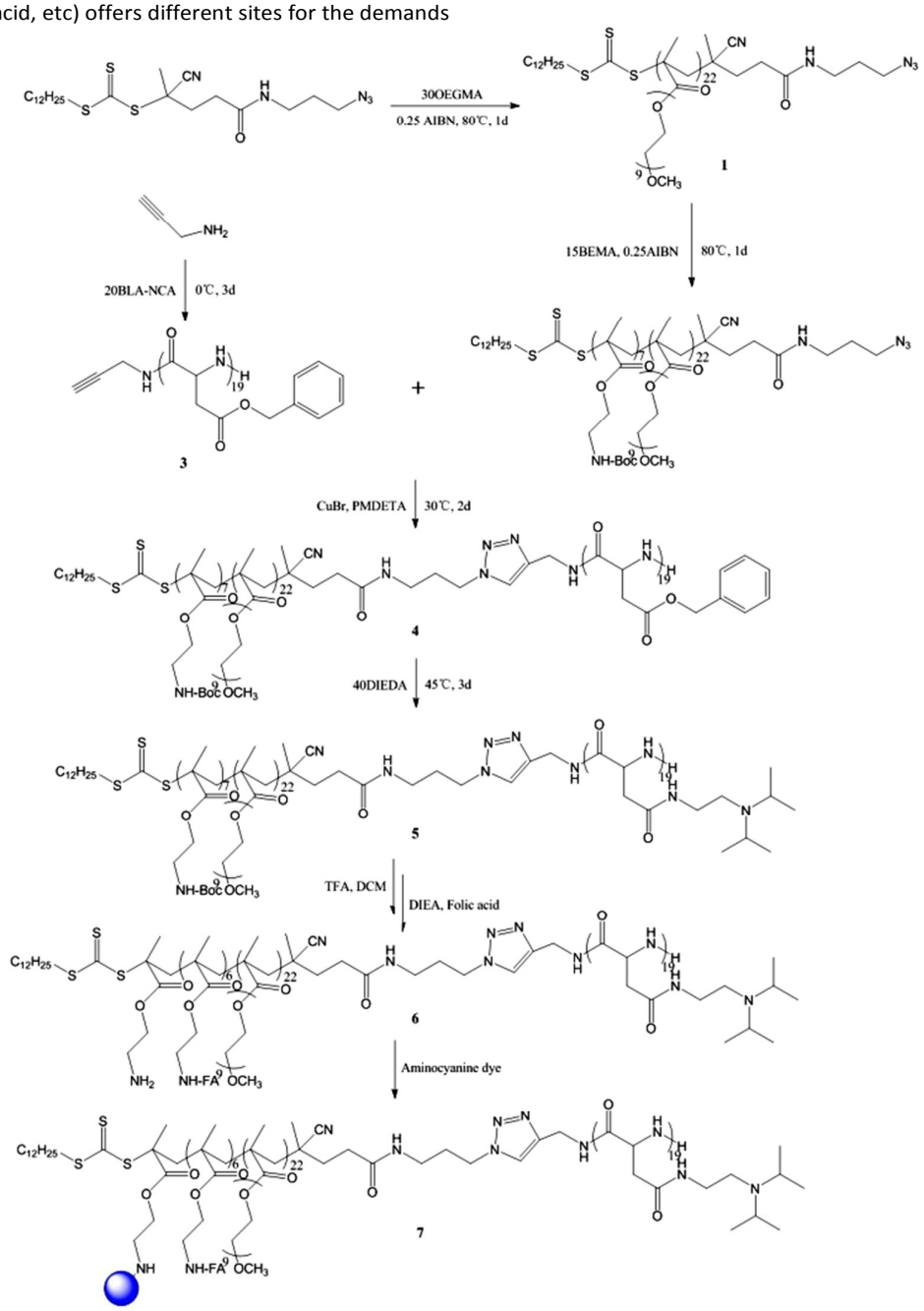

Scheme 2. Synthesis of the Folic acid Targeted, pH-Responsive and Near-Infrared Triblock Amphiphilic Polymer *via* Polymerization and Click Reaction.

Here, a novel triblock amphiphilic polymer has been designed and synthesized by a combination of Reversible Addition-Fragmentation Chain Transfer Polymerization (RAFT Polymerization), ROP and the Click Reaction (Scheme 2). The polymer is divided into two parts (the hydrophilic part and the hydrophobic one) to synthesize separately. To insure the water-solubility, the molecular weight of the hydrophilic part should be large enough with a ratio between 1:1 and 2:1 against the hydrophobic one according to our works before[12,21,22]. Here, an azido modified RAFT agent was used as the initiator for the radical polymerization. 22 units of Oligo(ethylene glycol) methacrylate (OEGMA) were polymerized to it with the same function as the traditional hydrophilic Polyethylene glycol (PEG). Subsequently, 7 units of t-butyloxy carbonyl (Boc) protected ethanolamine modified methacrylate (BEMA) were inserted between the trithiocarbonate and POEGMA to offer a binding site for the folic acid and fluorescence probe. The number of folic acid conjugated to the polymer should not be too much. Overmuch

View Article Online
DOI: 10.1039/C6RA05657A

folic acid would increase the hydrophobicity of the polymer and insufficient FA would decrease the effect of targeting. In another way, 10% molar ratio of fluorescence probe was linked to the polymer to get a high quantum yields avoiding the self-quenching[22]. For the hydrophobic part, since the benzyloxy group could be aminolyzed by hydrazine or amine for functionalization, β-benzyl-L-aspartate was selected to be polymerized to the initiator of propargylamine. Although the hydrazone bond is widely used for the pH-responsive drug delivery of doxorubicin, this style of chemical bonding has poorer ability of drug loading and is less sensitive to the stimuli compared to the physical encapsulation. According to this, the strategy of the response mechanism was changed from chemical bonding to physical encapsulation to fulfil the demands of rapid stimuli-response and drug release. So here, N,N-diisopropylethylenediamine was used for aminolyse, and the alkalinity of tertiary amino responded to the weak acidic microenvironment at the pH of about 6.3 in the amphiphilic system. 19 units of β-benzyl-L-aspartate were polymerized to propargylamine to ensure the ability of stimuli-response. If the number was less than 10, the micelles wouldn't change a little against the variation of the pH in the environment. After conjugation with Click Reaction, activated folic acid and a cyanine dye which is a near infrared (NIR) fluorescence probe were linked to the amino group on the block of PBEMA by covalent bonds following the de-protection of the Boc group. The doxorubicin was encapsulated accompanied with the formation of micelles. In normal neutral condition, micelles could keep a tight and stable structure and thus protect the drug in the micelles core. When in the tumoral acidic condition, the ionization of the tertiary amino group would contribute to the swell or collapse of micelles and the encapsulated doxorubicin would be released rapidly.[23-25]

Three kinds of polymers with NIR probe, namely, targeting polymers (TPs), nontargeting polymers (NPs) and polymers without drugs (PWDs) were synthesized and characterized. Two kinds of cancer cells, MCF7 and HepG2, were selected to study the effect of target and uptake of folic acid in different tumor environments.

Results and Discussion

Synthesis of the Monomer 2-(N-tert-butoxycarbonylamino)ethyl Methacrylate

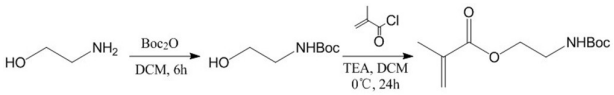

Scheme 3. Synthesis of the monomer, 2-(N-tert-butoxycarbonylamino)ethyl Methacrylate.

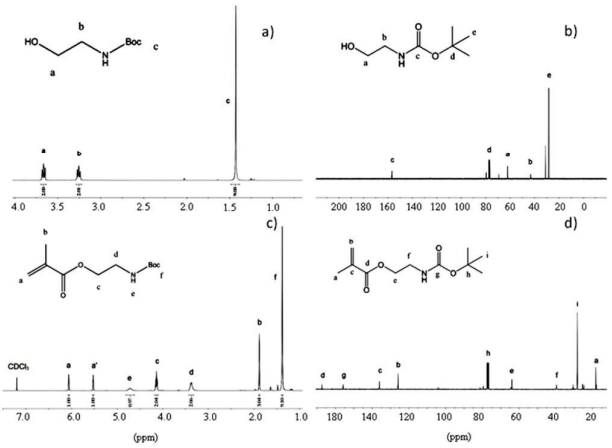

Figure 1. ^{1}H-NMRand ^{13}C-NMR spectra of 2-(N-tert-butoxycarbonylamino)ethan-1-ol in $CDCl_3$ (a, b), and 2-(N-tert-butoxycarbonylamino)ethyl Methacrylate in $CDCl_3$ (c, d).

This monomer was synthesized by two steps (Scheme 3). Since the final product needed to be purified by gel chromatography, the intermediate material, 2-(N-tert-butoxycarbonylamino)ethan-1-ol, was simply processed after reaction without further purification. Figure 1 shows the typical ^{1}H-NMR and ^{13}C-NMR spectra of the intermediate 2-(N-tert-butoxycarbonylamino)ethan-1-ol and the final monomer, and the peaks representing each hydrogen atom could be found in (a) and those for carbon atoms in (b). Due to the different chemical environment, the peaks of the cis form and the trans form hydrogen atoms on the double bond split to different chemical shifts, which were represented by a and a' (Fig.1c). It was found that all the hydrogen atoms could be corresponded to the peaks in the spectrum and the integration equalled the number of the atoms. The ^{13}C-NMR spectrum also indicated the correct structure of the final product (Fig.1d).

Synthesis of the Hydrophilic Part

Figure 2a showed the ^{1}H-NMR spectrum of $POEGMA_{22}$ in $CDCl_3$. Since there were various hydrogen atoms in different chemical environments, many peaks corresponding to hydrogen atoms overlapped and could not be integrated respectively. Some characteristic peaks representing different parts were chosen to identify the structure and the degree of polymerization. The peak at the chemical shift of 4.17 ppm represented the hydrogen atoms *f* on the methylene just next to the oxygen atom, whose ratio of integration to the peak b, and the middle 18 hydrogen atoms of the dodecyl, was about 44:18, illustrating that 22 units of OEGMA were polymerized to the RAFT initiator on the average.

Due to the fact that the reactive activity of the monomer, 2-(N-tert-butoxycarbonylamino)ethyl Methacrylate, was lower than the OEGMA monomer, more feed ratio or longer reaction time was needed for the polymerization. 15 times of BEMA was used as the reagent, as shown in Fig.2b, the integration of peak e+h was 58 which indicated that totally 29 units of BEMA and OEGMA were conjugated to the RAFT agent, indicates only 7 units were inserted between the trithiocarbonate and units

View Article Online
DOI: 10.1039/C6RA05657A

of OEGMA during 1 day, which gave the final structure with $PBEMA_7$-b-$POEGMA_{22}$.

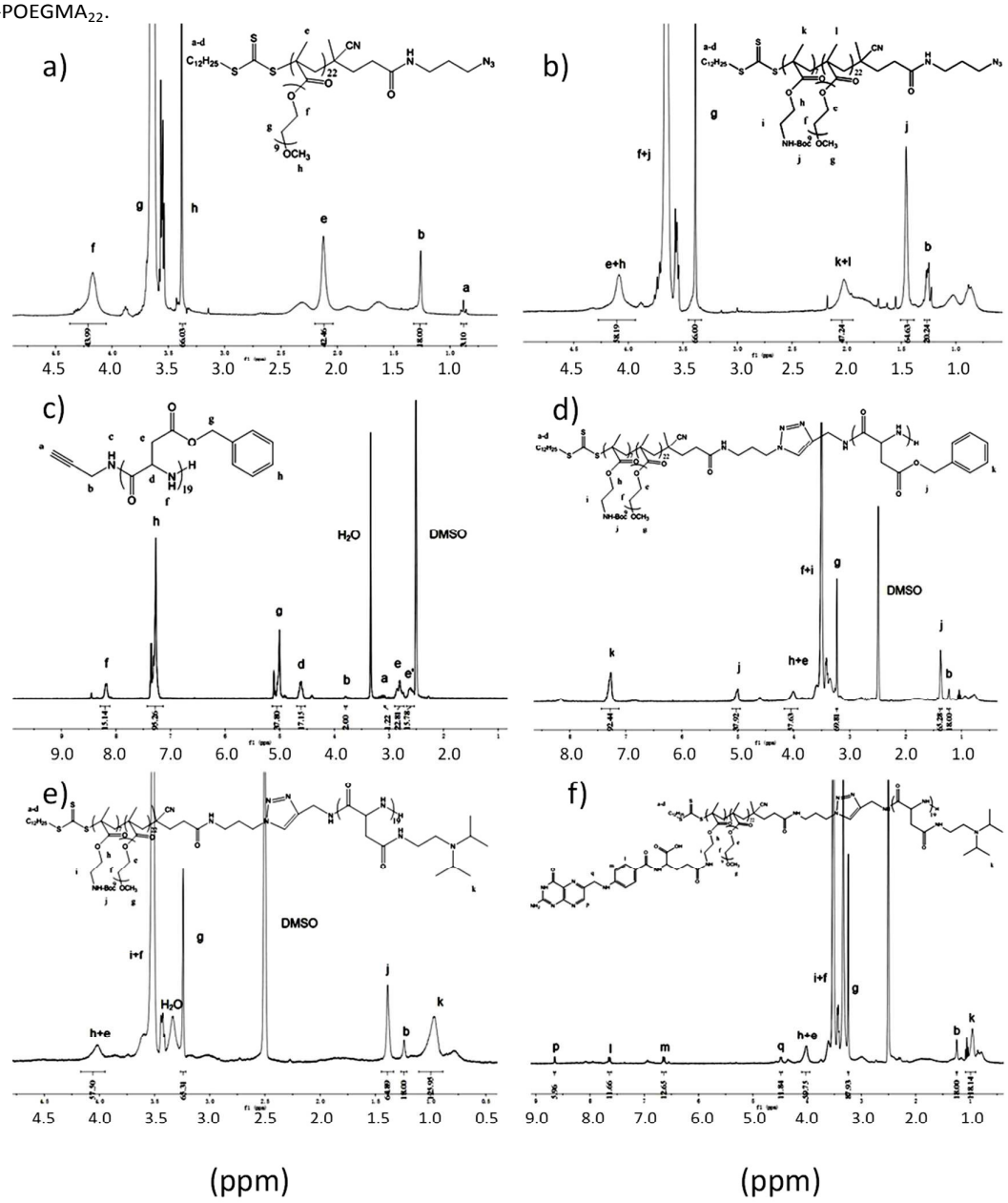

Figure 2. ^{1}H-NMR spectra of $POEGMA_{22}$ (a), $PBEMA_7$-b-$POEGMA_{22}$ (b), $PBLA_{19}$ (c), $PBEMA_7$-b-$POEGMA_{22}$-b-$PBLA_{19}$ (d), $PBEMA_7$-b-$POEGMA_{22}$-b-$P(Asp\text{-}DIEDA)_{19}$ (e), and folic acid conjugated polymer (f): (a) and (b) were measured in $CDCl_3$ while (c)-(f) were measured in DMSO-d^6.

View Article Online
DOI: 10.1039/C6RA05657A

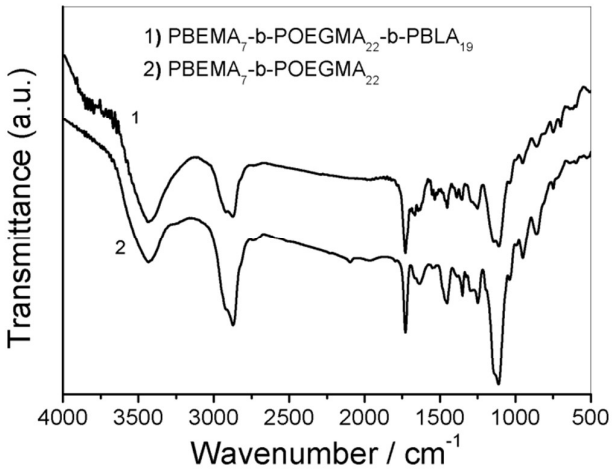

Figure 3. FT-IR spectrum of $PBEMA_7$-b-$POEGMA_{22}$ and $PBEMA_7$-b-$POEGMA_{22}$-b-$PBLA_{19}$.

Synthesis of the Hydrophobic Part

Figure 2c displayed the ^{1}H-NMR spectrum of the propargylamine initiated poly β-benzyl-L-aspartate (PBLA). The peak at 3.8 ppm corresponding to the hydrogen atoms on the methylene next to the triple bond was selected as the standard for the integration. The area of peak h and g which representing the number of the benzyl group indicated that about 19 units of the protected aspartic acid were polymerized to the initiator.

Synthesis of $PBEMA_7$-b-$POEGMA_{22}$-b-$PBLA_{19}$ by Click Reaction

The hydrophilic and hydrophobic parts were efficiently conjugated by Click reaction. As shown in Fig.2d, the characteristic peaks of $PBLA_{19}$ at 5.0 and 7.2 ppm and those of $PBEMA_y$-b-$POEGMA_{22}$ at 3.2 and 4.0 ppm could be observed and the ratio of the integration indicated the same proportion of the hydrophilic and hydrophobic segments. Its symmetrical size distribution and no existence of any shoulder peak which was displayed in Figure 4a illustrated the complete reaction of the reagents, and the disappearance of the peak at 2100 cm^{-1} in the FT-IR spectrum (Figure 3) also demonstrated the thorough completion of the reaction.

Aminolysis of the Triblock Polymer

To ensure the completion of aminolysis, excess N,N-diisopropylethylenediamine was used as the reagent to de-protect the benzyl group. As shown in Fig.2d, the disappearance of the peak at 5.0 and 7.2 ppm and the rise of the peak at 0.97 ppm indicated the successful conversion from benzyl group to terminal tertiary amino group. However, due to some unknown reason for the macromolecular polymer, it seemed that the integration of the methyl group was not very accurate. The integration of peak k was only about 126, which was less than the actual number of the hydrogen atoms. The same phenomenon appeared in the ^{1}H-NMR spectra of $POEGMA_{22}$ and $PBEMA_7$-b-$POEGMA_{22}$. In Fig. 2a, the integration of peak e representing the methyl on the main chain was less than the actual number of 66. And in Fig.2b, this peak became wider and the integration did not increase much after the polymerization of BEMA.

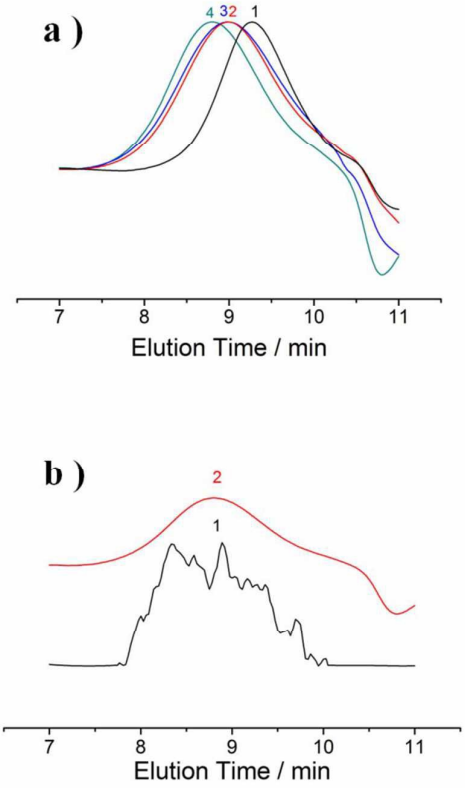

Figure 4. (a) GPC traces of (1, black) $PBLA_{19}$, (2, red) $POEGMA_{22}$, (3, blue) $PBEMA_7$-b-$POEGMA_{22}$ and (4, green) $PBEMA_7$-b-$POEGMA_{22}$-b-$PBLA_{19}$ in DMF measured by the RI detector. (b) GPC traces of the final Cy conjugated polymer (2) by fluorescence detector (Excited at 650 nm and Emitted at 790 nm compared with that by RI detector (1).

Addition of Folic acid, Cyanine Dye and Doxorubicin

Figure 2e showed the ^{1}H-NMR spectrum after the de-protection of the Boc group and the addition of folic acid. The disappearance of the peak at 1.45 ppm indicated the successful leaving of Boc group, and the integration of peak p, l, m and q illustrated that about 6 folic acids were conjugated to the terminal amino groups leaving one for the linkage with Cy.

Due that little cyanine dye and doxorubicin were conjugated and encapsulated respectively to the polymer, hardly any peaks of them could be found in the ^{1}H-NMR spectrum. In order to demonstrate the conjugation of Cy, GPC with fluorescence detector was used to characterize the product. As shown in Figure 4b, the traces representing the cyanine dye have the same elution time with the triblock polymer 4, which indicated that Cy had been successfully conjugated to the final polymer.

Polydispersity Index and Size Distribution

View Article Online
DOI: 10.1039/C6RA05657A

The polydispersity index and size distribution were measured by GPC and DLS in Fig.4 and Fig.S1, respectively (Table 1). As shown in Fig.4a, all the intermediate polymers had a satisfactory polydispersity index without any shoulder peaks indicating that all of them had a suitable molecular weight distribution, and larger molecular weight led a shift to lower elution time. The valley at 11min was the solvent peak.

The results of DLS were displayed in Fig.S1 in the Supporting Information. All of the TP, NP and PWD were in narrow size distribution with a size diameter around 108, 106 and 115 nm, respectively. The zeta potential of the polymers was also measured, which were 3.4, 7.3 and 8.4 mV for TP, NP and PWD, respectively, indicating that they had positive charge which was beneficial for the endocytosis by cells.

Micellce Stability

Since the zeta potentials of the particles were positive, the measurements of stability were carried out. Fig.S3 and Table S1 in the Supporting Information showed the stability of TP, NP and PWD micells in 10% serum solution. For each sample, the size distribution hardly changed in the experiment. In another way, the diameter kept the same within 24 h, while at 36 h, the value increased indicating the swell of the micelle. The micelles might be unstable in the serum solution as the time went on, however, they would keep a satisfactory stability within a favorable time.

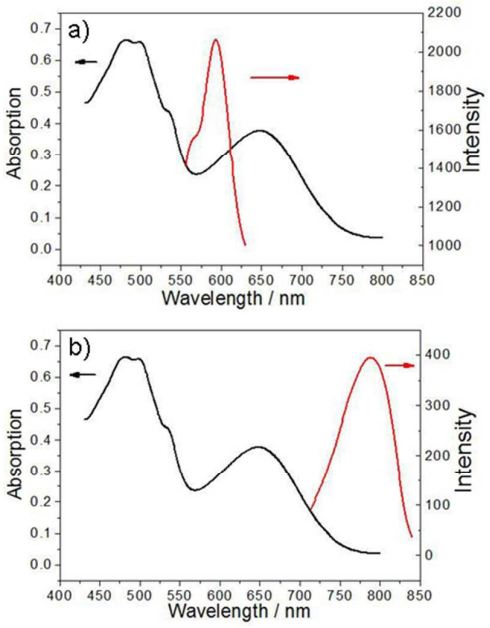

Figure 5. Absorption (black line) and emission (red line) curves of the TP (a) excited at 480 nm and (b) excited at 650 nm. The excitation and emission slit widths were 10 and 10 nm.

Table 1. Molecular weights and polydispersity indexes of the polymers.

Sample	M_n^{NMR}	M_n^{GPC}	M_w/M_n (PDI)
$POEGMA_{22}$	11485	12681	1.12
$PBEMA_7$-b-$POEGMA_{22}$	13089	14821	1.16
$PBLA_{19}$	3950	4572	1.05
$PBEMA_7$-b-$POEGMA_{22}$-b-$PBLA_{19}$	17039	19256	1.22

Optical Properties of the Polymer

The UV-vis and fluorescence spectra were measured to characterize the optical properties of TP which was shown in Fig.5. Two absorption peaks corresponding to doxorubicin and Cy could be observed at the wavelength of 480 and 650nm, and their emission peaks were at 590 and 790nm, respectively.

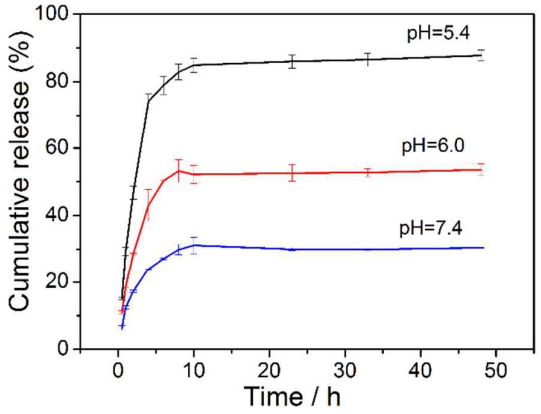

Figure 6. Drug delivery behavior of the targeted polymers under neutral (pH = 7.4), weak acidic (pH = 6.0) and acidic (pH = 5.4) conditions.

Drug Release

The in vitro drug delivery behavior were studied under normal neutral condition (pH 7.4), intracellular weak acidic environment (pH 6.0) and the environment in endosomes of tumor cells (pH 5.4), respectively. As shown in Fig.6, the polymeric nanoparticles was very sensitive against the acidic environment. Doxorubicin encapsulated in the micelles were released rapidly and subsequently accessed into a balance within 8 h. In order to better understand the behavior of the release, the size transformation of the micelles was measured by means of DLS, as shown in Fig.7. Under normal cellular condition, the micelles were kept in a stable status with the diameter around 100nm (Fig.7a), and little doxorubicin might leak out from them. This was why 30% of the drug would be delivered to the neutral environment with a little longer time. As the condition became weak acidic, the micelle expanded to a larger diameter of 115nm, 137nm, 328nm and 514nm with wider size distribution at pH 6.8, 6.6, 6.2 and 5.8, respectively. So the gaps of the micelles became larger, and the drug was easier to seep which showed a better behavior in delivery. At the pH of about 5.4, the original micelles began to collapse and irregular accumulation appeared. This is why a large quantity of doxorubicin can be released to the environment and rapidly reached the balance.

View Article Online
DOI: 10.1039/C6RA05657A

RSC Advances

ARTICLE

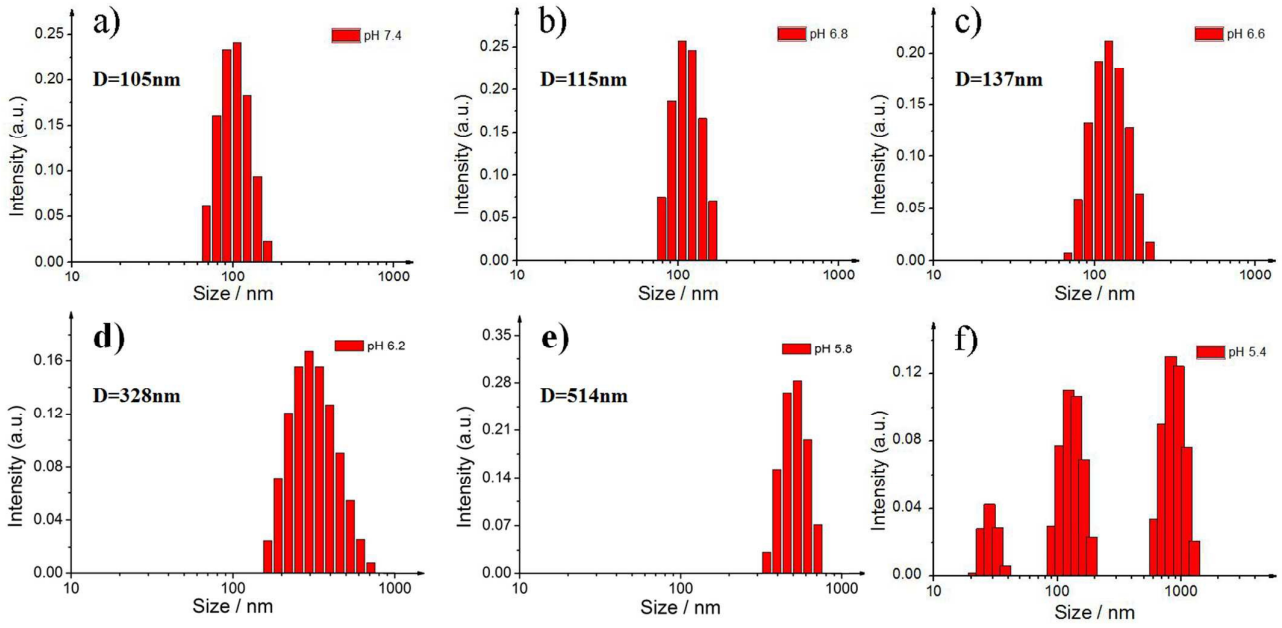

Figure 7. The transformation of the size and size distribution of targeted polymers with the decrease of pH.

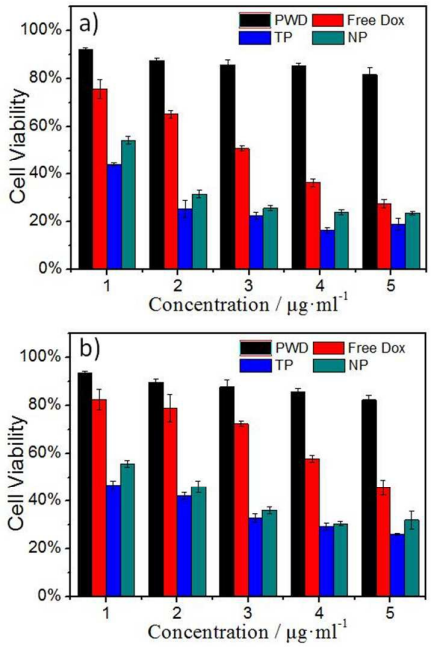

Figure 8. Cytotoxicity of TP (navy), NP (dark cyan), PWD (black) and free doxorubicin (red) in MCF7 (a) and HepG2 (b) cells.

Cytotoxicity

The MTT method was utilized to study the cytotoxicity of TP, NP and PWD against the MCF7 and HepG2 cells, respectively. Keeping the concentration of doxorubicin encapsulated in the micelle consistent, the cell survival ratio was measured under gradient concentration, and the concentration of PWD was kept the same with that of TP. The results were shown in Fig. 8. In both MCF7 and HepG2 cells, more than 80% cells cultivated with polymers without drug still alive, indicating the low toxicity of the polymer itself. Since these two kinds of cells both had overexpressed folate receptors on their surface, cells incubated with TPs had lower survival ratio than those with NPs under different concentration. Beyond that, another two phenomena should be paid attention. Firstly, at the same level of concentration, polymers with drug had better performance than the free doxorubicin. This might be not only contributed to the effect of folic acid, but also because that the polymers with a positive charge on their surface were easier to be endocytosed by cells leading a better effect of the drug. Secondly, this diversity and the differences between TP and NP decreased as the concentration increased. It could be illustrated that the function of folic acid and the polymer was just synergic. At a low concentration or in a short time, they would improve the endocytosis of the cells and the effect of drugs, while the concentration increased to a particular level, the drug would be easily endocytosed and the function of them would not express obviously. The values of IC50 were

View Article Online
DOI: 10.1039/C6RA05657A

also calculated, which were 33 μg/mL and 47 μg/mL for TP and NP when MCF7 cells were used and were 42 μg/mL and 52 μg/mL for TP and NP when HepG2 cells were used.

Cellular Uptake Study

Both the MCF7 and HepG2 tumor cells were cultivated with polymers of consistent concentration of doxorubicin for 24 h. At predetermined time (2 h, 6 h, 12 h, 24 h), the cells were observed by the fluorescence microscope after staining the cell nuclei with DAPI. The images of the fluorescence microscope were shown in Fig.9 and Fig.S2. For all the cells cultivated for 12 h and 24 h, the images were captured with the exposure time of 200 ms. While for the cells of 6 h, images of 200 ms were too dim to recognize, which might because nanoparticles accumulated as time went on and there were fewer micelles at 6 h. In the same way, the exposure time for cells of 2h should be extended to 930 ms to obtain pictures bright enough. It was apparent that images of 24 h were brighter than those of 12 h indicating higher concentration of polymeric nanoparticles. So it could be concluded that as the extension of the cultivated time, more polymers were endocytosed by the cells. The trace of the polymers without drug could be observed in Fig.9c and Fig.S2c. It could be found that hardly any macromolecule gathered in the nuclei, while they just dispersed all around in a random condition.

Cells cultivated with TP and NP showed the similar phenomena in the aggregation of doxorubicin. As shown in all Fig.9a, 9b, and Fig.S2a and S2b, almost all of the fluorescence emitted by doxorubicin which increased as the cultivated time extended appeared in the region of nuclei (displayed in line Merge 1), while a little presented nearby. Considering the treatment mechanism of doxorubicin, the released DOX finally gathered in the nuclei, and the undelivered ones would coincide with the macromolecule which could be well implied by the images. From another aspect, it marched with the results of drug delivery. Due to the great sensitivity of physical wrapping compared with chemical connection, the micelle would rapidly collapse after entering the intracellular environment of tumor cells at the pH of about 5.4 and the doxorubicin encapsulated could be released immediately.

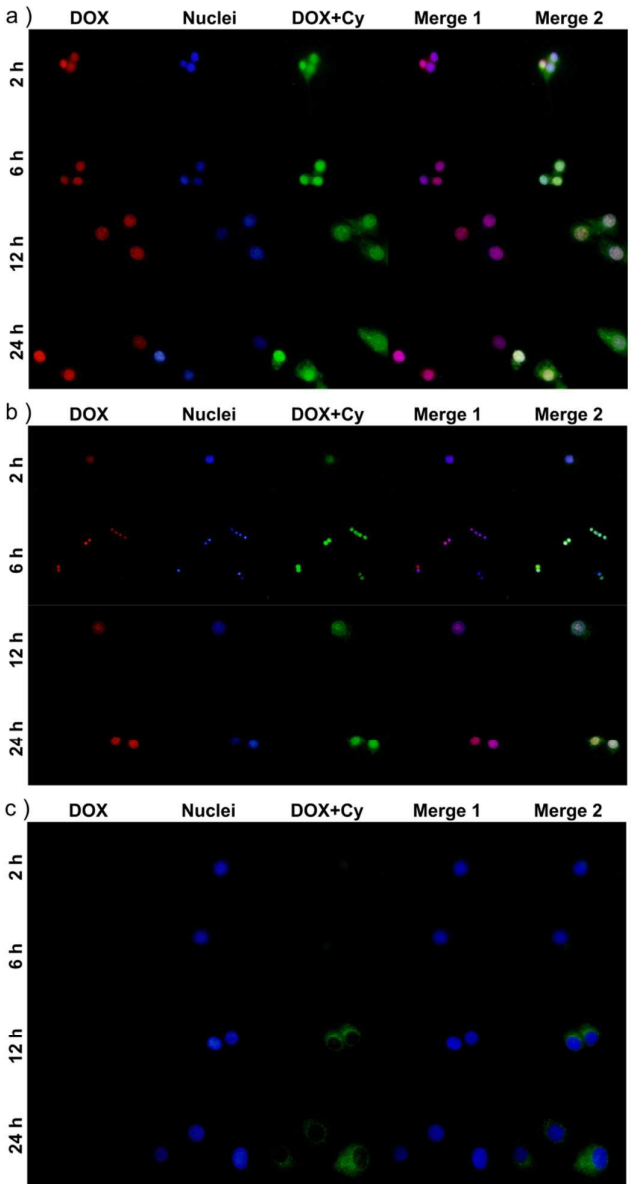

Figure 9. Images of fluorescence microscope of MCF7 cells cultivated with (a) TP, (b) NP and (c)PWD for 2 h, 6 h, 12 h and 24 h, respectively.

Both for MCF7 and HepG2 cells, treating with TPs displayed stronger fluorescence at each time point compared with those treated with NPs. This phenomenon is consistent with the results of cytotoxicity. In a short time of cultivation, the interaction between folic acid and folate receptor would observably improve the endocytosis of the polymers by cells leading a better utilization of drugs.

Flow cytometry

In order to further prove the uptake of TP was much higher than that of TP, measurements of flow cytometry were carried out. As shown in Fig.10, higher mean fluorescence intensity (MFI) could be observed in the MCF7 cells cultivated with TP indicating a more population of DOX-positive cells for TP than

View Article Online
DOI: 10.1039/C6RA05657A

those of NP. The result corresponded with those of cytotoxity and cellular uptake study, collectively illustrating that the folic acid would improve the endocytosis of the polymers by tumor cells.

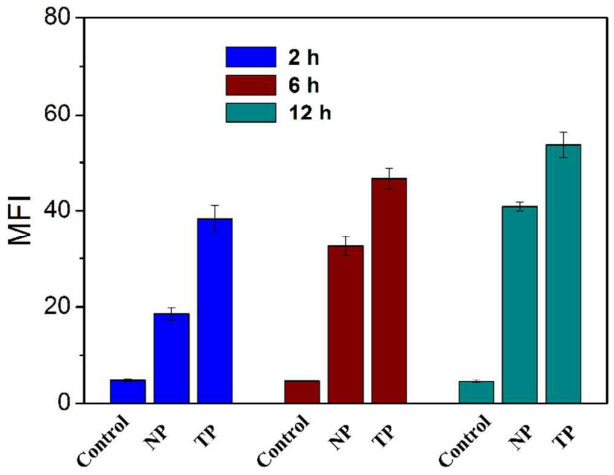

Figure 10. DOX-positive cell populations measured by flow cytometry of MCF7 cells cultivated with TP and NP at 37°C for 2 h (blue), 6 h (wine) and 12 h (dark cyan).

Experimental Section

Materials

Unless specifically indicated, the chemical reagents used in the experiments were purchased from Sinoreagent Corporation. Azodiisobutyronitrile (AIBN), oligo(ethylene glycol) methacrylate (OEGMA, M_w=500), methacryloyl chloride, propargylamine, β-benzyl-L-aspartate, triphosgene, N,N,N',N',N'-pentamethyldiethylene triamine (PMDETA), folic acid, N,N'-dicyclohexyl carbodiimide (DCC), N-hydroxysuccinimide (HOSu), doxorubicin hydrochloride, diisopropylethylamine (DIEA) were purchased from Aladdin Corporation, China. N,N-diisopropylethylenediamine was purchased from Tokyo Chemical Industry (TCI) Corporation, Shanghai, China. Roswell Park Memorial Institute (RPMI), 4'6-diamidino-2-phenylindole (DAPI) was purchased from Invitrogen, Carlsbad. Dulbecco modified eagle medium (DMEM), fetal bovine serum (FBS) and methyl thiazolyl tetrazolium (MTT) were obtained from Sangon Corporation, China. The normal phase column chromatography process used 200-300 mesh silica gel (Yantai Institute of Chemical Engineering, China). The dialysis bags (cut off M_w = 1000, 3000 and 7000) were purchased from Jinsui Bio-Technology Corporation, Shanghai, China. Tetrahydrofuran (THF) and n-hexane were dried by with CaH_2 under reflux overnight and distilled. Anhydrous N,N-dimethylformamide (DMF) was obtained by stirring with CaH_2 at room temperature for 2 days followed by vacuum distillation. The ultrapure water was prepared using a Milli-Q Synthesis System (Millipore).

Synthesis of the RAFT-APA

This material was prepared according to another work which was done by ourself.[12]

Synthesis of APA-RAFT-POEGMA$_{22}$

225mg (0.464 mmol) RAFT-APA, 19.0mg AIBN (0.116 mmol 0.25 equiv) and 6.96g OEGMA (M_w=500, 13.9 mmol 30 equiv) were dissolved in 2 mL DMF in a Schlenk tube under an argon gas atmosphere. The mixture was stirred at 80°C for 24 h and then purified against ultrapure by dialysis. Followed by freeze-drying, 4.85g yellow solid (91.1% yields) was obtained.

Synthesis of 2-(N-tert-butoxycarbonylamino)ethan-1-ol

In a 250 mL round-bottom flask, 2.24g (36.7 mmol) 2-aminoethan-1-ol was dissolved in 20mL DCM, followed with the addition of 8.0g Boc_2O (36.7mol, 1 equiv) in 10 mL DCM dropwise at 0°C. The mixture was reacted at room temperature for 4 h. After filtration, the solvent was removed by reduced pressure distillation. 5.38g (91.0% yields) of product was obtained as transparent liquid. ^{1}H-NMR (300 MHz, $CDCl_3$) δ 3.64 (t, J = 5.1 Hz, 2H), 3.23 (t, J = 5.1 Hz, 2H), 1.41 (s, 9H). ^{13}C-NMR (75 MHz, $CDCl_3$) δ 156.77 (s), 78.12-75.48 (m), 62.03 (s), 43.19 (s), 28.36 (s).

Synthesis of 2-(N-tert-butoxycarbonylamino)ethyl Methacrylate

3.0g 2-(N-tert-butoxycarbonylamino)ethan-1-ol (18.6 mmol) and 2.82g triethylamine (27.7 mmol, 1.5 equiv) were dissolved in 20 mL dry DCM in a 100 mL round-bottom flask. 3.1g methacryloylchloride (29.8 mmol, 1.6 equiv) was dropped into the solution in an ice bath and the mixture was stirred at 0°C for 24 h. After filtration and removing the solvent by reduced pressure distillation, the raw product was purified via column chromatography (petroleum ether/ethyl acetate, 10:1 v/v). Removing solvent and vacuum drying gave 3.7g white solid, yielding 86.7%. ^{1}H-NMR (300 MHz, $CDCl_3$) δ 6.06 (s, 1H), 5.53 (s, 1H), 4.72 (s, 1H), 4.14 (t, J = 5.3 Hz, 2H), 3.38 (t, J = 5.3 Hz, 2H), 1.88 (s, 3H), 1.38 (s, 9H). ^{13}C-NMR (75 MHz, $CDCl_3$) δ 167.28 (s), 155.80 (s), 136.00 (s), 125.92 (s), 78.29-75.64 (m), 63.93 (s), 39.67 (s), 28.33 (s), 18.28 (s).

Synthesis of PBEMA$_7$-b-POEGMA$_{22}$

In a Schlenk tube, 800mg $POEGMA_{22}$ (0.070 mmol), 2.9mg AIBN (0.018 mmol, 0,25 equiv) and 239mg BEMA (1.04 mmol, 15 equiv) were dissolved in 4 mL DMF. After reacted at 80°C for 24 h, the solution was sealed in dialysis bag and dialyzed against water. Removing the water by freeze-drying gave 720mg white solid, yielding 78.9%.

Synthesis of BLA-NCA

This proceed was the same as our another work.[12]

Synthesis of PA-PBLA$_{19}$

To a flame-dried Schlenk tube purged with argon, 11.1mg propargylamine (0.201 mmol) was mixed with 5 mL dry DMF. After cooled to 0°C in an ice bath, 1.0g BLA-NCA (4.02 mmol, 20 equiv) dissolved in 10 mL DMF was added into the tube.

View Article Online
DOI: 10.1039/C6RA05657A

The solution was reacted at 0°C for 3 days and at room temperature for 12h. After dialysis against ultrapure water, the white precipitation was filtered and washed with water. Freeze-drying gave 710 mg powder, yielding 89.2%.

Synthesis of $PBEMA_7$-b-$POEGMA_{22}$-b-$PBLA_{19}$ by Click Reaction

A 4 mL DMF solution containing 497mg $PBEMA_7$-b-$POEGMA_{22}$ (38 μmol) and 150mg $PBLA_{19}$ (38 μmol, 1 equiv) was added to a Schlenk tube. After adding 5.5mg CuBr (38 μmol, 1 equiv) and 6.6mg PMDETA (38 μmol, 1 equiv) into the system, the reaction was carried out under argon gas atmosphere at 30°C for 2 days. The solution was purified by dialysis against an aqueous solution containing EDTA. After removing the water by freeze-drying, 512mg yellow solid (79.1% yields) was obtained.

Aminolysis of the Triblock Polymer

In a flame-dried Schlenk tube, 440mg $PBEMA_7$-b-$POEGMA_{22}$-b-$PBLA_{19}$ (25.8 mmol) was dissolved in 3 mL anhydrous DMF. 149mg N,N-diisopropylethylenediamine (1.03 mol, 40 equiv) was added to the solution under argon atmosphere. The mixture was heated to 45°C and stirred for 3 days. Following dialysis, freeze-drying gave 380mg yellow solid (83.0% yields).

Activation of Folic Acid

300mg folic acid (680 mmol) and 78.2mg HOSu (680 mmol, 1 equiv) was dissolved in 5 mL DMSO. After cooled to 0°C, 1 mL DMSO solution containing 156mg DCC (814 mmol, 1.2 equiv) was added. The mixture was stirred for 24 h and prepared for the next step without any further treatment.

Deprotection of Boc and Conjugation of Folic Acid

350mg $PBEMA_7$-b-$POEGMA_{22}$-b-$P(Asp\text{-}DIEDA)_{19}$ (19.7 mmol) was dissolved in a mixed solvent of 1 mL TFA and 2 mL DCM. After stirred for 6 h, the solvent was removed by reduced pressure distillation. The obtained oily solid was dissolved into 2 mL DMF, followed by the addition of 66mg N,N-diisopropylethylamine (512 mmol, 26 equiv) and 1.22 mL of the FA-NHS (138 mmol 7equiv) solution prepared above. It was stirred at room temperature in the dark for 12 h. The solution was purified by dialysis against water. After freeze-drying, 312mg yellow solid (80.3% yields) was obtained.

Conjugation of Cyanine Dye and Encapsulating Doxorubicin

Amino modified cyanine dye was synthesized as it mentioned in our previous work.[12] 5mg aminocyaine dye (5.73 μmol), 0.8mg HOSu (6.95 μmol, 1.2 equiv) and 1.4mg DCC (6.79 μmol, 1.18 equiv) were dissolved in 1 mL dry DMF. After stirred for 24 h, 300 μL of it was added to 2 mL DMF containing 200mg polymer 6. The solution was reacted for 12 h.

15mg doxorubincin hydrochloride (25 mmol) was dissolved in 1 mL DMF and neutralized by 3.8mg triethylamine (TEA) (37.5mmol, 1.5 equiv). It was stirred for 5 min and then added to the solution prepared above. After mixing uniformly, the mixture was sealed in a dialysis bag and was dialyzed against water for 1 day. The micelle was obtained.

NP was synthesized without the conjugation of Folic acid and PWD was obtained without the encapsulation of DOX.

The drug loading rate was measured by using UV spectrophotometer at the wavelength of 480nm. After compared with a UV standard curve made by ourselves, the ratio of drug weight to polymer weight was 3.0% for TP and 2.7% for the NP.

All the reactions in this part were carried out in the dark.

Characterization

Deuterated chloroform and deuterated dimethyl sulfoxide containing 0.03 vol% tetramethylsilane (TMS) were used as the solvent for the measurements of ^{1}H-NMR and ^{13}C-NMR spectra by using a Bruker AC 300 spectrometer. A Shimadzu UV-2401 PC Ultraviolet was used to measure the UV-vis spectra. Shimadazu RF-5301PC fluorescence spectrophotometer was used to measure the fluorescence intensity with the excitation and emission slit widths of 10 and 10nm. FT-IR spectra were obtained by using a Bruker EQUINOX 55 Fourier transform-infrared spectrometer with the KBr disk method. The molecular weights and PDI of the polymers were measured by gel permeation chromatography (GPC, LC-20AD, Shimadzu) which was equipped with a refractive index detector (RID-10A), a Shodex GPC KD-804 column, and a spectrofluorometric detector (RF-20Axs, Shimadzu). DMF was used as the mobile phase and monodispersed standard polystyrene samples to calibrate the value of M_n, Mw and Mw/Mn. Dynamic light scattering (DLS, Malvern Zetasizer Nano ZS90 with He-Ne laser and 90o collecting optics) was used to measure the size and size distribution of the micelle solution. The absorbance for MTT cytotoxicity was measured using the Bio-rad iMak microplate reader. The fluorescence microscope measurements were carried out on Olympus U-HGLGPS. The results of the flow cytometry were measured on a FACSCalibur flow cytometer (BD Biosciences) and then analyzed with BD FACSCalibur flow cytometer.

Micellce Stability

200 μL of the three micelle solutions (10 mg/mL) were added to 1 mL 10% serum aqueous solutions and were kept for 2 h, 12 h, 24 h, 36 h, respectively. Then 0.1 mL of the solution was taken out for the measurement of DLS.

In vitro Drug Delivery

The performance of drug delivery was measured both in neutral and acidic microenvironments. For the neutral condition, 500 μL micelle solution (10 mg/mL) was sealed in a dialysis bag and then immersed in 50 mL PBS solution (pH 7.4) at 37°C on a shaking bath. At each predetermined time point, 2 mL of the PBS solution was removed and isopyknic fresh PBS solution was added. The delivery quantity of doxorubicin was calculated by testing the fluorescence intensity of emission wavelength at 577nm with an excitation wavelength at 480nm.

View Article Online
DOI: 10.1039/C6RA05657A

For the acidic condition, PBS (pH 6.0) and acetate buffer (pH 5.4) was used as the release media instead.

Size Transformation of the Micelles in Acidic Condition

20 mL TP micellces solution was kept at 37°C in a 100 mL beaker. 0.1 M HCl aqueous solution was used to adjust the pH to several predetermined point. After balance, 0.1 mL of the solution was taken out to measure the size and size distribution by DLS.

Cytotoxity

The cytotoxity of the polymers was measured with a methyl tetrazolium (MTT) viability assay against MCF7 and HepG2 cells. Experiments in both the cells were carried out in a similar way. In short, cells were seeded in 100 μL DMEM in 96-well plates at the density of 3000 cells per well, followed by incubation for 24 h. After replacing DMEM, different concentrations of free Dox or the three kinds of polymers we synthesized were added. Following cultivation for 24 h, 20 μL MTT with the concentration of 5 mg/mL was added to each well and incubated for another 4 h. Then the plates were shaken for 10 min with the addition of 150 μL DMSO. The absorption of the wells was measured at 570nm.

Cellular Uptake Study

MCF7 cells were seeded on in 500 μL DMEM in 12-well plates at a density of 10^5 cells per well. They were cultivated at 37°C for 24 h. After discarding the culture medium, polymers with consistent concentration of doxorubicin dissolved in 500 μL DMEM was added. Then the cells were cultivated for 2 h, 6 h, 12 h and 24 h. Following labelling the cell nuclei with DAPI, the cells were observed with a fluorescence microscope.

Flow Cytometry

For flow cytometric analysis, MCF-7 cells were seeded into 24-well plates at 5×10^4 cells per well in 0.5 mL of complete RPMI-1640 medium at 37°C in a 5% CO_2 humidified atmosphere for 24 h. The original medium was replaced with nanoparticles at an equivalent dose of 4 μg/mL Dox per well. The cells were incubated 2 h, 6 h, 12 h at 37°C and were then rinsed twice with cold PBS. The cells were trypsinized, washed twice with cold PBS, and resuspended in cold PBS for flow cytometric analysis using a BD FACSCalibur flow cytometer.

Conclusions

A novel folic acid targeted triblock amphiphlic polymer has been synthesized with the combination of RAFT polymerization, Ring-opening polymerization and Click reaction. The nanosized micelles of the polymer has low toxicity and are easily endocytosed by tumor cells with overexpressed folate receptors on their surface. They are sensitive to the change of the pH value in the microenvironment and would expand and collapse for rapid drug delivery, which could kill the targeted tumor cells in a short time. The conjugation of a NIR dye to the polymer makes it a theranotic agent for the imaging-guided drug delivery, and this kind of novel polymer is potential for the future cancer treatment.

Acknowledgements

This work is supported by the National Natural Science Foundation of China (No. 51373162), and the Natural Science Foundation of Anhui Province (No. 1408085MKL03).

Notes and references

‡ Footnotes relating to the main text should appear here. These might include comments relevant to but not central to the matter under discussion, limited experimental and spectral data, and crystallographic data.

1. Z. Zhang, J. Wang, X. Nie, T. Wen, Y. Ji, X. Wu, Y. Zhao and C. Chen, *J. Am. Chem. Soc.*, 2014, **136**, 7317-7326.
2. O. Veiseh, J. W. Gunn and M. Zhang, *Adv. Drug Deliver. Rev.*, 2010, **62**, 284-304.
3. M. S. Shim and Y. J. Kwon, *Adv. Drug Deliver. Rev.*, 2012, **64**, 1046-1059.
4. S.-H. Kim, J.-K. Kim, S.-J. Lim, J.-S. Park, M.-K. Lee and C.-K. Kim, *Eur. J. Pharm. Biopharm.*, 2008, **68**, 618-625.
5. S. M. Sharker, S. M. Kim, S. H. Kim, I. In, H. Lee and S. Y. Park, *J. Mater. Chem. B*, 2015, **3**, 5833-5841.
6. L. Fan, Y.-J. Fu, Q.-L. Liu, D.-T. Lu, C. Dong and S.-M. Shuang, *Chem. Commun.*, 2012, **48**, 11202-11204.
7. S. A. Hilderbrand, K. A. Kelly, M. Niedre and R. Weissleder, *Bioconjugate. Chem.*, 2008, **19**, 1635-1639.
8. H. Zhang, J. Fan, J. Wang, S. Zhang, B. Dou and X. Peng, *J. Am. Chem. Soc.*, 2013, **135**, 11663-11669.
9. M. Zhang, B.-C. Yin, W. Tan and B.-C. Ye, *Biosens. Bioelectron.*, 2011, **26**, 3260-3265.
10. K. Park, S. Lee, E. Kang, K. Kim, K. Choi and I. C. Kwon, *Adv. Funct. Mater.*, 2009, **19**, 1553-1566.
11. M. K. Yu, J. Park and S. Jon, *Theranostics*, 2012, **2**, 3.
12. L. Fu, C. Sun and L. Yan, *ACS Appl. Mater. Interfaces*, 2015, **7**, 2104-2115.
13. C. Sun, R. Sze and M. Zhang, *J. Biomed. Mater. Res. A*, 2006, **78**, 550-557.
14. Y. Liu, K. Li, J. Pan, B. Liu and S. S. Feng, *Biomaterials.*, 2010, **31**, 330-338.
15. G. Pasut, F. Canal, L. Dalla Via, S. Arpicco, F. M. Veronese and O. Schiavon, *J. Control Release*, 2008, **127**, 239-248.
16. H. Shmeeda, L. Mak, D. Tzemach, P. Astrahan, M. Tarshish and A. Gabizon, *Mol. Cancer Ther.*, 2006, **5**, 818-824.
17. J. Cheng and T. J. Deming, in *Peptide-based materials*, Springer, 2012, pp. 1-26.
18. N. Hadjichristidis, H. Iatrou, M. Pitsikalis and G. Sakellariou, *Chem. Rev.*, 2009, **109**, 5528-5578.
19. T. J. Deming, *Chem. Rev.*, 2016, **116**, 786-808.
20. H. Schlaad, in *Peptide hybrid polymers*, Springer, 2006, pp. 53-73.
21. T. Xing and L. Yan, *RSC Advances*, 2014, **4**, 28186-28194.

View Article Online
DOI: 10.1039/C6RA05657A

22. T. Xing, B. Lai, C. Mao and L. Yan, *J. Control Release*, 2013, **1**, e50.
23. Y. Li, G. H. Gao and D. S. Lee, *J. Polym. Sci. Pol. Chem.*, 2013, **51**, 4175-4182.
24. S. J. Hwang, M. S. Kim, J. K. Han, D. S. Lee, B. S. Kim, E. K. Choi, H. J. Park and J. S. Kim, *Macromol. Res*., 2007, **15**, 437-442.
25. C. Y. Zhang, Y. Q. Yang, T. X. Huang, B. Zhao, X. D. Guo, J. F. Wang and L. J. Zhang, *Biomaterials*., 2012, **33**, 6273-6283.